CHAPTER 7

REFRACTOMETRY

"Eigentlich weiss man nur wenn man wenig weiss, mit dem Wissen wächst der Zweifel."
("We know accurately only when we know little; with knowledge doubt increases.")
Goethe

7.1 REFRACTIVITY OF AIR

When performing length interferometry in air, it is important to correct the laser wavelength for the refractivity of the air through which it passes. The correction factor, the refractive index, is applied to the vacuum wavelength of the light emitted by the laser

$$\lambda = \frac{\lambda_{vac}}{n} \tag{7.1}$$

where λ is the wavelength in air, λ_{vac} is the wavelength in vacuum, and n is the refractive index of air, for the ambient conditions.

The refractivity [1] of a gas, (n-1), can be expressed as the product of 2 factors: the dispersion factor K_λ and the density factor D_{TP}. The dispersion factor depends only on the wavelength and the density factor is independent of the wavelength. Hence

$$(n-1)_{TP} = K_\lambda D_{TP} \tag{7.2}$$

7.1.1 Dispersion factor

Svensson [2] demonstrated the invariance of the dispersion factor with temperature and Erickson [3] demonstrated its invariance with pressure. Due to this invariance, the dispersion factor can easily be determined to high accuracy by relative measurement, and in 1953 the dispersion formula was published by Edlén [4], based on the work of other authors' investigations.
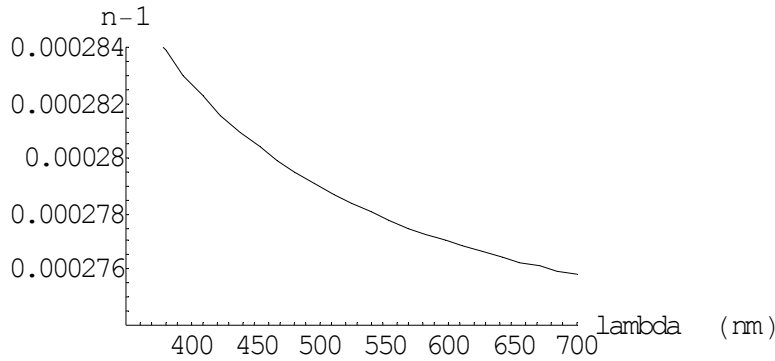
Figure 7.1 - *Dispersion of standard air over the region 350 nm - 700 nm*

This formula for the dispersion factor was expressed in the Sellmeier form

$$(n-1) = \sum_i A_i \frac{1}{\sigma_i^2 - \sigma^2} \qquad (7.3)$$

The σ_i represent wave-numbers of certain resonance frequencies, σ is the experimental wave-number. This is the basic form of the more recent dispersion formula (see below) that is now used. The Sellmeier formula is based on the idea that the refractivity of air is due to discrete absorption frequencies. This can be modelled by using Maxwell's equations in a dielectric medium in which an electric field interacts with an idealised harmonic oscillator, with various resonant frequencies. This is, however, not quite correct, as these absorption bands are not discrete frequencies, but continua. The term with the constant 38.9 in the formula below represents the effect of the absorption continuum of O_2, peaking at 145 nm, with a range of 40 nm. The constants 130 and 8342.13 represent the effect of the absorption continua of N_2 and O_2, starting at 100 nm, levelling off at 50 nm, before tailing off for lower wavelengths. Thus there is an empirical equation for K_λ , the dispersion factor, based on measurements of the dispersion of air.

7.1.2 Density factor

Edlén [5] gives a derivation for the density factor, D_{TP} based on the Lorentz-Lorentz equation, and the gaseous equation of state

$$\frac{PV}{RT} = 1 - \varepsilon_T P \qquad (7.4)$$

and measured values of $\dfrac{PV}{RT}$ for dry air at different conditions. The form of the derived equation is

$$D_{TP} = \frac{P(1 + \beta_T P)}{(1 + \alpha T)} \tag{7.5}$$

This corresponds to equation (7.7) below relating the refractivity of air at non-standard pressures and temperatures, to that at standard conditions.

7.2 EDLÉN'S EQUATIONS FOR THE REFRACTIVITY OF AIR

In 1965 Edlén reviewed the most recent work [6,7], collated findings and issued new formulae for the dispersion of air [5]. The formulae derived in that paper have since been widely used to correct for the refractivity of air, with a minor correction to the humidity term suggested by Birch and Downs [8].

7.2.1 Refractivity of standard air

According to Edlén, standard air (dry air at 1 atmosphere, 15°C, containing 300 ppm by volume of CO_2) has a refractivity of

$$(n-1)_s \times 10^8 = 8342.13 + \frac{2406030}{130 - \sigma^2} + \frac{15997}{38.9 - \sigma^2} \tag{7.6}$$

where n is the refractive index, σ is the vacuum wave-number in μm^{-1}. As an example, for air at 15 °C, $\lambda = 633$ nm, $(n-1)_s = 0.000\ 276\ 517$.

This is found to be accurate to about 1×10^{-8} over the wavelength range from 200 nm to the infra red, and represents the dispersion factor, described above.

7.2.2 Corrections for temperature, pressure, water vapour and CO_2

The effects of temperature and pressure are calculated from the density factor

$$(n-1)_{TP} = (n-1)_s \times \frac{P}{720.775} \left[\frac{1 + P(0.817 - 0.0133T) \times 10^{-6}}{1 + 0.0036610\,T} \right] \tag{7.7}$$

where P is the air pressure in torr, and T is the air temperature in °C. At 1 atmosphere (1013.25 mbar, 760 torr) and 20 °C, $(n-1)_{TP} = 0.000\,271\,786$.

A correction can also be applied for water vapour (humidity)

$$n_{TPf} = n_{TP} - f\left(5.722 - 0.0457\sigma^2\right)\times 10^{-8} \tag{7.8}$$

for air containing f torr of water vapour.

Birch and Downs [8] suggest an amendment to the last equation, whereby it becomes

$$n_{TPF} = n_{TP} - f\left(3.7209 - 0.0343\sigma^2\right)\times 10^{-8} \tag{7.9a}$$

but with f in mbar, not torr. When converted for measurements of f in torr, the wavelength-dependent term is unchanged from Edlén and the equation becomes

$$n_{TPF} = n_{TP} - f\left(4.9608 - 0.0457\sigma^2\right)\times 10^{-8} \tag{7.9b}$$

This is to correct an error in the water vapour term discovered using an absolute gas refractometer. Muijlwijk [9] suggested alterations to the standard formulae, on the grounds that normal laboratory conditions are now typically 20 °C, and 400 ppm by volume of CO_2. However, he acknowledged the fact that the equations that he presented agreed with Edlén's original equations to within 1 part in 10^8, and thus for reasons of standardisation with other existing instruments, the refractivity equations used in the work of this thesis are those due to Edlén, 1966, with the Birch and Downs modification to the humidity term. The Birch and Downs revised humidity term has been verified by Beers and Doiron [10].

Birch and Downs expect the uncertainty of their modified Edlén equations to be $\pm 3 \times 10^{-8}$ unless more accurate measurements of the pressure, temperature and humidity are made. The amount of Carbon Dioxide must also not deviate from the standard value of 300 ppm by volume, unless its value is measured directly, as is the case with the NPLBI.

The effect of CO_2 concentration on the refractivity, according to Edlén, is given by

$$(n-1)_x = \left[1 + 0.540(x - 0.0003)\right](n-1)_s \tag{7.10}$$

where x is the CO_2 concentration, by volume. The effects of other gases commonly found in the atmosphere are negligible, unless specific contamination is introduced.

7.3 EFFECTS OF PRESSURE, TEMPERATURE, HUMIDITY AND CO_2 ON REFRACTIVITY

Table 7.1 summarises the effects of the air temperature, pressure, water vapour content (humidity) and CO_2 content on the refractive index.

Parameter	Typical value	Typical daily variation in calibration laboratory	Effect of variation on refractive index
temperature	20 ° C	± 0.2 °C	∓ 1.85 x 10^{-7}
pressure	1013.25 mbar	± 20 mbar	± 5.36 x 10^{-6}
humidity	13 mbar	± 2 mbar	∓ 5.45 x 10^{-8}
CO_2 content	300 ppm	± 100 ppm	± 1.47 x 10^{-8}

Table 7.1 - *Typical variations in air temperature, pressure, humidity and CO_2 content*

Thus air pressure and temperature have the largest effect on the refractive index, hence accurate measurement of these parameters is essential if the refractive index is to be calculated accurately using Edlén's equations.

Parameter	Increment	Effect on refractive index
temperature	1 ° C	-9.26 x 10^{-7}
pressure	1 mbar	2.68 x 10^{-7}
humidity	1 mbar	-2.73 x 10^{-8}
CO_2 content	100 ppm	1.47 x 10^{-8}

Table 7.2 - *Effect of air temperature, pressure, humidity and CO_2 content on refractivity*

7.3.1 Pressure measurement

The pressure transducer used in the PLBI is a Druck DPI 140. This instrument has a range of 35 - 1150 mbar (absolute), with a resolution of 0.01 mbar. The manufacturer's estimated accuracy of the instrument is ± 0.02% of reading ± 0.01% of full scale, or approximately ± 0.23 mbar, though with direct calibration against NPL primary standards, an estimated uncertainty of ± 0.08 mbar can be achieved.

The DPI 140 is situated in the equipment rack and is connected via a tube to the chamber. The opening of the tube is positioned on the carriage, close to the length bars,

ensuring that the pressure sense point is close to the measurement beam. To prevent the pump used to sample the chamber air from affecting the pressure, it is switched off before the pressure readings are made. The DPI reading is available over the IEEE bus, and is read by the computer, which applies a software correction to the reading according to the latest calibration.

The DPI works by measuring the resonant frequency of an oscillating cylinder, which is dependent on the density of the air surrounding the cylinder, which in turn is dependent on the air pressure. The measurement is thus a measurement of density and is affected, to second order, by humidity and other gaseous contaminants. The effect of these has been minimised by the used of the sealed chamber, situated in a humidity-controlled laboratory. From the manufacturer's handbook, it is seen that the errors given in table 7.3 arise in the pressure reading due to a change from 0% Relative Humidity (RH) to 70%, at the stated temperatures.

Temperature (°C)	Error (% reading)	Error at 1 atm (mbar)
10	0.004	0.04
25	0.010	0.10
30	0.013	0.13

Table 7.3 - *Errors in pressure reading due to change from 0% to 70%RH*

7.3.2 Temperature measurement

The temperature of the air inside the chamber is measured *in situ* by a platinum resistance thermometer. The PRT is enclosed in a small heatsink, placed on an insulating support, close to the length bars. The PRT thus measures the temperature of the air within a small region, which requires the temperature along the measurement beam to be uniform. An alternative would be to use many PRT sensors along the path, but the extra time taken to measure these sensors (approximately 20 seconds each) would allow drift of the readings of temperature and pressure and thus outweigh the advantage of having more measurement points. The temperature gradients along the beam paths are very small and do not affect the air temperature measurement: when the chamber is temperature-controlled at 20 °C, the temperature gradient along the measurement path has been measured as less than 0.001 °C per metre, and hence only one temperature measurement is required. The drift rate is less than 0.002 °C per hour.

The resistance of the PRT is measured using a Tinsley Senator 5840D precision AC resistance bridge which is based on an NPL design. The bridge uses a series of computer-switched precision transformer windings to balance the voltage in the two

arms of a Wheatstone bridge. The decade-windings are switched in or out according to the voltage difference between the two arms. The 1:1 windings are used first, followed by the 10:1, then the 100:1 and so on, gradually decreasing the out-of-balance signal. A digital display can be configured to show either the resistance reading, resistance ratio to an external standard resistor, or temperature calculated by an external computer, connected via the IEEE bus, along which the resistance reading or an out-of-balance indicator signal can be sent.

The PRT resistance is measured in a 4-terminal configuration to account for the resistance of the cables. The bridge contains a standard resistor, which is temperature controlled. The resolution of the bridge is 0.000 01 ohms, corresponding to a temperature resolution of 0.000 03 °C. When calibrated against an external 100 ohm standard resistor, the accuracy of the bridge is estimated to be ± 0.000 47 °C (0.47 mK).

Each PRT used with the bridge is individually calibrated at the water triple point and the melting point of gallium, 0.01 °C and 29.7646 °C, respectively. The uncertainties in the realisations of these standard temperatures are ± 0.000 5 °C and ± 0.000 5 °C, respectively. Calibration of the resistance of the PRTs at these temperatures allows calculation of corresponding resistance-temperature coefficients according to the International Temperature Scale of 1990 (ITS-90). Following a measurement of the resistance of a PRT, the ITS-90 coefficients allow the corresponding temperature to be calculated to within an accuracy of 0.000 13 °C (see § 8.3).

7.3.3 Humidity measurement

The water vapour content (humidity) of the air is measured by a Michell S3000 dewpoint hygrometer. This device measures the dewpoint of air passing over a temperature-controlled mirror by controlling the temperature of the mirror to the point where dew forms on its surface. A photocell senses the intensity of light reflected from the mirror surface - this signal decreases when dew forms on the mirror. The temperature of the mirror is monitored by a PRT. A simple formula [**11**] is used to convert the dewpoint temperature, T_{dp}, into a partial pressure of water vapour, f, in mbar.

$$f = \log^{-1}\left(\frac{7.5 \times T_{dp}}{237.3 + T_{dp}} + 0.78571 \right) \tag{7.10}$$

The resolution of the S3000 is 0.1 °C dewpoint and is calibrated against traceable humidity standards to provide an accuracy of ± 0.25 °C. The dewpoint reading is converted into a voltage which is read by a DVM with an IEEE interface. Overall accuracy of humidity measurement is estimated to be ± 0.3 °C (± 0.24 mbar vapour pressure).

Due to the heat output of the peltier cooler attached to the dewpoint mirror, the sensor is mounted outside the chamber. Air is sampled from the chamber from a point near the length bars by a PTFE-coated re-circulating pump. The air flows along PTFE/stainless steel tubes, through the S3000 sensor, through the CO_2 sensor, and is returned to the chamber. The pump surfaces are PTFE and are sufficiently clean for analytical gas sampling operations and hence do not contaminate the returned air. The flow rate of the sampled air is approximately 0.5 litres min^{-1}.

7.3.4 Carbon dioxide measurement

The CO_2 content of the sampled air is measured using an Edinburgh Instruments GASCARD CO_2 sensor. This measures the relative absorption of light passing through a sample tube of gas. The sampled gas flows through a single chamber, approximately 10 cm long, though which a wide-band light source shines. The intensity detected at certain wavelengths is used to provide an output signal (monitored by an IEEE DVM) which corresponds to the CO_2 molar density. The instrument has a resolution of ± 18 ppm CO_2 and an uncalibrated accuracy of ± 60 ppm. The device is calibrated using standard gases at 0 ppm and 370 ppm (by volume) to achieve an estimated accuracy of ± 30 ppm.

7.3.5 Air parameter measurement order

The measurements of air temperature, pressure, humidity and CO_2 concentration are performed at the same time as the phase-stepping measurements. The order of the individual measurements is given below. The order of measurement of devices is designed so that parameters which are slowly varying (humidity, CO_2, bar temperature) are read at the start and end of the measurement, whereas more quickly varying parameters (air pressure and temperature) are read at the same time as the phase-stepping is performed. The CO_2 and humidity readings are taken before the sample pump is temporarily halted.

(1)   The air temperature PRT is selected.

(2)   The humidity sensor is read by the computer.

(3)   The CO_2 sensor is read by the computer.

(4)   The sample pump is stopped.

(5)   The air temperature PRT is read.

(6)   One of the two PRTs for measuring the temperature of the length bar is read.

(7)   The phase-stepping is performed at three wavelengths.

(8)   The air pressure is read by the computer.

(9)   The second bar temperature PRT is read.

(10)   The sample pump is re-started.

From the measurements of pressure, temperature, humidity and CO_2 content, the refractivities at the three measurement wavelengths are calculated using the modified Edlén equations. The wavelengths corrected for the effects of refractive index are used in the length calculation routine.

7.4 OTHER WAVELENGTH COMPENSATION TECHNIQUES

7.4.1 Two-wavelength compensation

Matsumoto and Honda [**12**] used a two-wavelength interferometer based around a YAG laser with a frequency-doubling crystal ($KTiOPO_4$) producing both 1.06 μm and 532 nm wavelengths. The interferometer averaged fringe counts at the two wavelengths to derive a wavelength-corrected fringe count which corresponded to the length being measured by the moving part of the interferometer. An accuracy of length measurement of 0.2 μm over 1 m of travel was obtained in air.

7.4.2 Gas refractometry

The refractive index of air can be measured directly in a gas refractometer. The refractive index, or the refractivity (the refractive index -1) of a sample of gas is measured relative to that of a known standard, often vacuum.

In order to check the accuracy of the results of the modified Edlén equation and as a possible second technique for refractive index determination, a gas refractometer was

constructed at NPL by Mr P D West, based on the design of the NPL Gas Refractometer of Birch and Downs [**13**,**8**].

7.4.2.1 Gas refractometer design

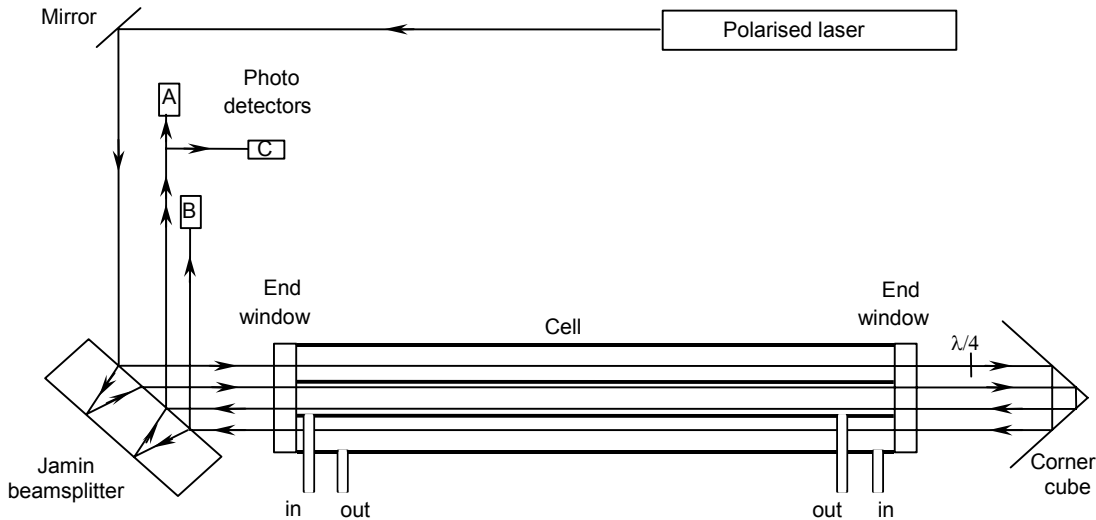The design of the refractometer is shown in figure 7.2.

Figure 7.2 - Gas refractometer schematic

This instrument is based around a polarised interferometer using a Jamin beamsplitter and a linearly polarised laser. A concentric two-chamber stainless steel gas cell with quartz end plates is used to contain the sample and reference gases. The inner cell is used for the reference, which is usually vacuum and the outer cell for the sample gas. The external solenoid valves and pipework allow interconnection of the two chambers allowing serial flow of the sample gas though both chambers, gas-outer & vacuum-inner, or both vacuum.

Vacuum is provided by a simple rotary pump (Edwards Model 1.5), which achieves a vacuum of 3 x 10^{-2} mbar. The three photo detectors are gain matched: two provide the orthogonal output signals from the interferometer, the third is used to adjust the gain of the other two detection channels, based on the intensity of the laser beam.

The internal length of the cell is approximately 316.6 mm, corresponding to 10^{6} interference fringes, at the laser wavelength, thus when comparing the optical path lengths of the two cell chambers, a difference in refractive index of 1 x 10^{-6} will be equivalent to 1 interference fringe. This is the basis of operation of the interferometer.

7.4.2.2 Refractometer operation

Sample gas is flowed though both chambers using the sampling pump for a period of 10 minutes. The pump is then switched off to allow the gas to stabilise at ambient pressure. A fringe counter, connected to two photocells which monitor the two orthogonal outputs of the interferometer, is zeroed. The sample pump is re-started and the inner chamber evacuated. As the air is removed, the change in refractive index causes a change in optical path length of the reference cell. The signals from two orthogonal outputs then exhibit a sinusoidal variation corresponding to the passage of interference fringes across the two detectors. The fringe counter tracks these fringes by tracking the two outputs.

When a sufficient vacuum has been obtained in the inner chamber, the display of the fringe counter will be the refractivity of the sample gas, with a factor of 10^{-6}. When a reading is required, the sample pump is stopped for 60 secs before the reading is taken. As an example, a fringe count of 267.123 corresponds to a refractive index of 1.000 267 123.

7.4.2.3 Corrections and errors

Due to constructional and operational constraints, a number of corrections have to be applied to the reading of the fringe counter to obtain the correct refractive index of the sample gas.

(1) Cell length

Due to engineering tolerances, the cell length is not exactly 1 million half-wavelengths long, thus the fringe count is first multiplied by a correction factor of 0.999716 (determined from accurate measurements of the cell length using a Co-ordinate Measuring Machine and a Gauge Block Comparator).

(2) Imperfect vacuum

The refractive index of absolute vacuum is 1 by definition. The refractive index increases by 2.7×10^{-9} per 10^{-2} mbar, thus due to the imperfect vacuum achieved by the rotary pump, a correction of 8.1×10^{-9} is added to the fringe count.

(3) Cell expansion

The cell is made of stainless steel which has a thermal expansion coefficient of 14.7×10^{-6} K^{-1}. Thus the cell length is dependent on temperature. A correction factor of 5×10^{-9} K^{-1} departure from 20 °C is applied to the fringe count.

(4) Gas adsorption

It has been shown [14] that when moist air is admitted to a previously evacuated cell in order to measure its refractivity, some water molecules are absorbed by the metallic walls of the cell, leading to a decrease in the humidity of the air with a corresponding increase in the refractivity of up to 1×10^{-7}. This effect can be removed by continuously flushing with ten cell volumes of gas, prior to making a measurement. Alternatively, the cell can be used in the reverse configuration with the two chambers of the cell initially flushed with air before one is evacuated (as used in the refractometer used with the NPLBI).

However, the process of physisorption [15] can still lead to an error. Here, water molecules in the stationary air are adsorbed onto the stainless steel wall, leading to an increase in the refractivity of up to 1.5×10^{-7}. The effect can be minimised by increasing the flow rate of the gas prior to stopping the flow for measurement and by reducing the overall size of the refractometer cell tubes.

(5) Pressure effects

Unless the pressures at the sample point and within the cell are equal, there will be a pressure-dependent refractivity gradient between these two points, and the refractivity measured by the refractometer will not be the same as that at the sample point. Thus, the effect of gravity on the air pressure must be taken into account, and the cell placed at the same height (above sea level) as the sample point. The earth's pressure gradient near the surface causes a change in refractive index of -3×10^{-8} m^{-1} ascent.

A second order pressure effect is due to the optical path length changes induced in the cell windows by the pressure change as air is evacuated from one of the cell chambers. For a 320 mm long cell, this has been shown [16] to cause a change in the measured refractivity of up to 1×10^{-8}.

(6) Temperature effects

The refractometer measures the refractive index of the gas under the conditions present inside the cell chamber. If there is a temperature gradient between the sample point and the cell, then the refractive index will be different at these two points and a correction factor, based on Edlén's equation will be required. When the length bar interferometer is being used to perform thermal expansion measurements, the temperature of the air inside the sealed chamber can be as high as 30 °C. The temperature of the air surrounding the refractometer is approximately 20 °C. The specific heat capacity of air is so low, that the air sampled from the interferometer chamber cannot supply enough energy to heat the refractometer cell by more than approximately 0.5 °C, and so a large temperature gradient exists between the chamber and the refractometer cell. This will cause a change in refractive index due to not only the temperature change (which can be measured) but also a possible change due to possible outgassing of the connection pipes or water condensation inside the cell, which cannot be measured.

(7) Fringe interpolation

As mentioned in section 2.3.1, errors arise in the fringe interpolation of the fringe counter due to effects such as gain mis-match between the two signals, offsets and phase errors. Some degree of computer correction is possible [17] by fitting ellipses to the data, although this takes time and requires low-noise signals. In the present refractometer, drift of the electronics or the alignment of the interferometer causes the offset and gain for the two channels to vary, leading to fringe interpolation errors.

7.4.2.4 Comparison between Edlén and refractometer

To compare the performances of the modified Edlén equations and the refractometer, they were both used to measure the refractive index of air sampled from the interferometer chamber.
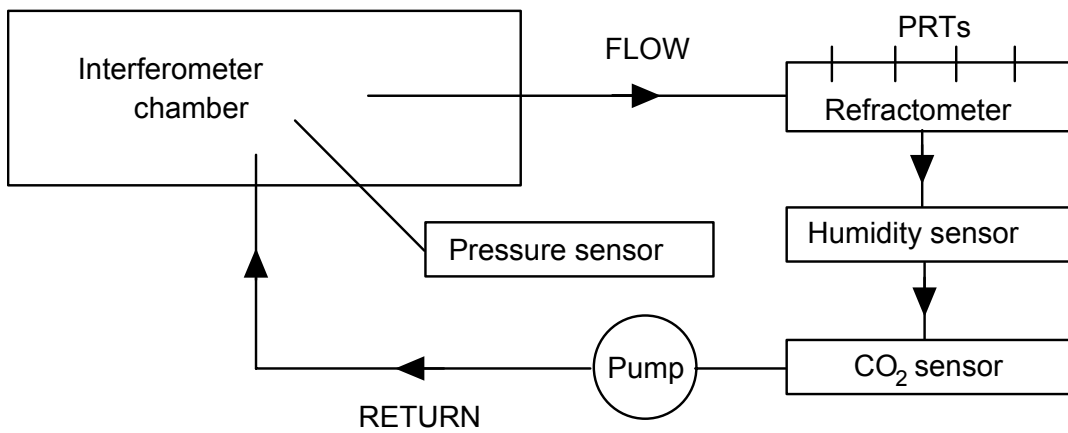
Figure 7.3 *- Comparison of Edlén and refractometer*

The value of the refractive index measured by the refractometer was compared against that calculated using the modified Edlén equation based on measurements of the air parameters. The air temperature used for the calculations was that inside the refractometer cell and the pressure was measured inside the interferometer chamber.

General agreement between the two methods was $\pm$ 3 x 10^{-8}, as can be seen in figure 7.4. On analysis of the data, it can be seen that the difference between the two methods is periodic with a period equal to one refractometer fringe, as shown in figure 7.5. This indicates that the two channels do not remain in perfect phase quadrature with equal offsets and gains. This was also detected by viewing the outputs of the two channels as a lissajous figure on an oscilloscope.
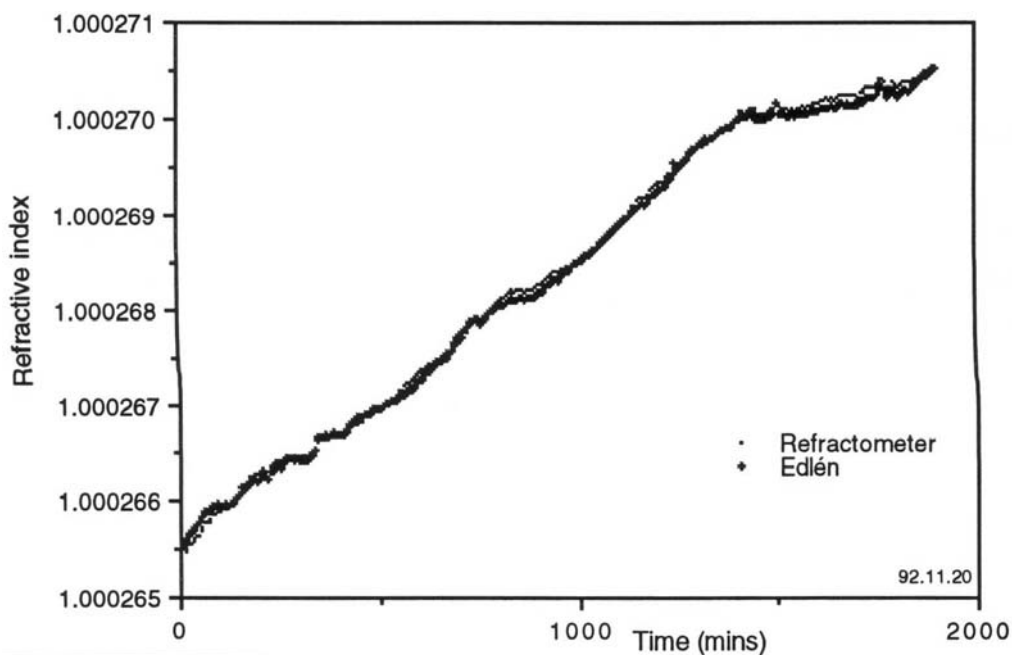

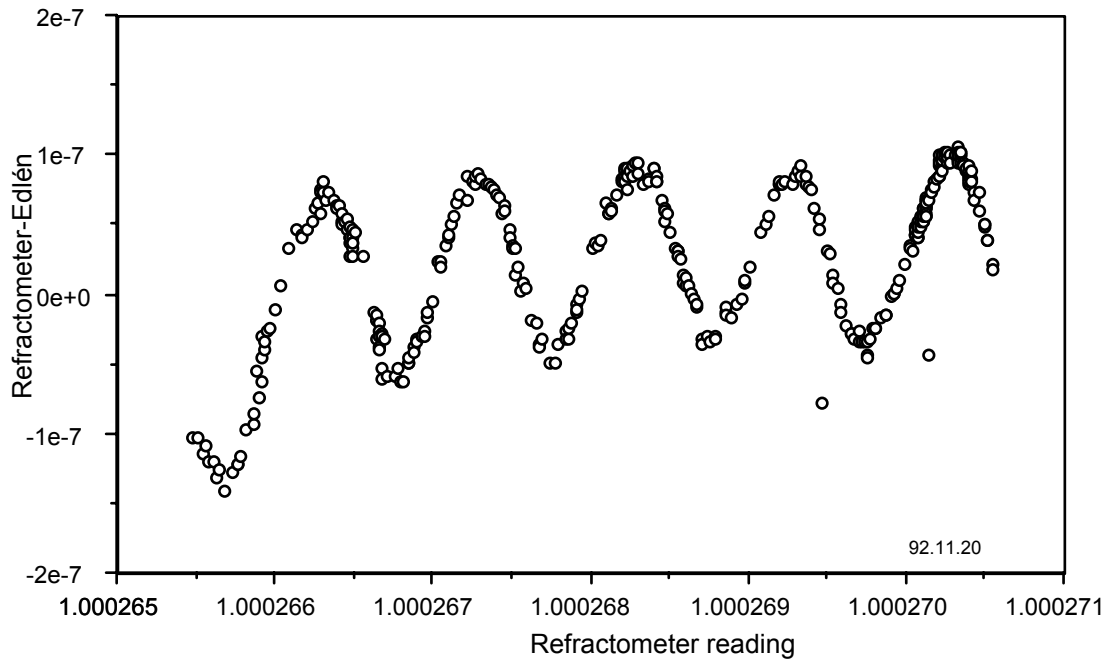***Figure 7.4*** *- Comparison of Edlén and refractometer*

Figure 7.5 - *Periodic error due to drift*

Thus although an absolute gas refractometer can be used to measure the refractive index of the air, the accuracy of measurement is generally no better than that achievable by the use of Edlén's equations coupled with sensitive, accurate transducers. Because of the fact that the composition of the air inside the chamber does not change rapidly, if at all, the calculation of the refractive index should be at least as accurate as the determination using the refractometer. At elevated temperatures, unless the system is re-designed with an internal refractometer, of a more stable design, Edlén is the only accurate solution to measure the refractivity of the air inside the interferometer chamber.

Birch *et al* [**18**] compared the results of air refractivity measurements made using an automatic refractometer with those obtained using commercial sensors and the Edlén equations. Their conclusion was that the modified Edlén equation is the most accurate form to use for calculating air refractivity. An uncertainty of $\pm$ 3 x 10^{-8} is achievable. When account is taken of excess CO_2 levels (above the nominal 300 ppm assumed by Edlén), the modified Edlén equation is accurate to about $\pm$ 1 x 10^{-8}.

7.5 ADDENDUM

Birch & Downs [19] have recently published updated Edlén equations for the refractive index of air. These new formulae take into account: the adoption of SI units (the pascal is now the recommended unit of pressure, not the torr); the establishment of the International Temperature Scale of 1990, superseding IPTS-68; improvements in the equation for the density of moist air [20]; increased CO_2 levels; and revision of the water vapour term. The new standard equations are as follows.

$$(n-1)_{TP} = \frac{P(n-1)_s}{96095.43} \times \frac{1+10^{-8}(0.601-0.00972T)P}{1+0.0036610T} \tag{7.11}$$

$$(n-1)_s \times 10^{-8} = 8343.05 + \frac{2406294}{130-\sigma^{-2}} + \frac{15999}{38.9-\sigma^{-2}} \tag{7.12}$$

$$n_{TPf} = n_{TP} - f(3.7345 - 0.0401\sigma^{-2}) \times 10^{-10} \tag{7.13}$$

where T is the temperature in °C, f is the water vapour pressure in Pa, σ is the wavelength in μm and P is the air pressure in Pa. These new formulae are expected to have an uncertainty, over the wavelength range 350 - 650 nm, of $\pm$ 1 x 10^{-8}. These equations will be incorporated into the software which calculates refractive index inside the interferometer.

[2002 re-publication note

Equation 7.12 has since been corrected by Birch & Downs to become:

$$(n-1)_s \times 10^{-8} = 8342.54 + \frac{2406147}{130-\sigma^{-2}} + \frac{15998}{38.9-\sigma^{-2}}$$

There have been several later revisions of these equations by other authors]

REFERENCES FOR CHAPTER 7

[**1**]   Barrel H & Sears J E   The refraction and dispersion of air for the visible spectrum *Phil. Trans. Roy. Soc. London* **A 238** (1939) 1-64

[**2**]   Svensson K   *Arkiv Fysik* **16** (1960) 361

[**3**]   Erickson K E   Investigation of the invariance of atmospheric dispersion with a long-path refractometer *J. Opt. Soc. Am.* **52** (1962) 777-780

[**4**]   Edlén B   The dispersion of standard air *J. Opt. Soc. Am.* **43** (1953) 339-344

[**5**]   Edlén B   The refractivity of air *Metrologia* **2** (1966) 71-80

[**6**]   Rank D H, Saksena G D & McCubbin T K   Measurements of the dispersion of air from 3651 to 15300 Angstroms *J. Opt. Soc. Am.* **48** (1958) 455-458

[**7**]   Peck E R & Khanna B N   Dispersion of air in the near-infrared *J. Opt. Soc. Am.* **52** (1962) 416-419

[**8**]   Birch K P & Downs M J   The results of a comparison between calculated and measured values of the refractive index of air *J. Phys. E: Sci. Instrum.* **21** (1988) 694-695

[**9**]   Muijlwijk R   Update of the Edlén formulae for the refractive index of air *Metrologia* **25** (1988) 189

[**10**]   Beers J & Doiron T   Verification of revised water vapour correction to the refraction of air *Metrologia* **29** (1992) 315-316

[**11**]   British Standard BS 1339 (1965) (London: British Standards Institution)

[**12**]   Matsumoto H & Honda T   High accuracy length-measuring interferometer using the two-colour method of compensating for the refractive index of air *Meas. Sci. Technol.* **3** (1992) 1084-1086

[**13**]   Downs M J & Birch K P   Bi-directional fringe counting interference refractometer *Precis. Eng.* **5** (1983) 105-110

[**14**]   Birch K P & Downs M J   Errors in the determination of the refractive index of air *Appl. Opt.* **28** (1989) 825-826

[**15**]   Birch K P, Downs M J & Ward R E   The measurement of humidity variations in gases resulting from the dispersion of water onto surfaces *J. Phys. E: Sci. Instrum.* **21** (1988) 692-694

[**16**]   Birch K P, Downs M J & Ferris D H   Optical path length changes induced in cell windows and solid etalons by evacuation *J. Phys. E: Sci. Instrum.* **21** (1988) 690-692

[**17**]   Birch K P   Optical fringe subdivision with nanometric accuracy *Precis. Eng.* **12** (1990) 195-199

[**18**]   Birch K P, Reinboth F, Ward R E & Wilkening G   The effect of variations in the refractive index of industrial air upon the uncertainty of precision length measurement *Metrologia* **30** (1993) 7-14

[**19**]   Birch K P & Downs M J   An updated Edlen equation for the refractive index of air   *Metrologia* **30** (1993) 155-162

[**20**]   Giacomo P   Equation for the determination of the density of moist air (1981) *Metrologia* **18** (1982) 33-40